Fluctuating radiocarbon offsets observed in the southern Levant and implications for archaeological chronology debates

Sturt W. Manning[a,1], Carol Griggs[a], Brita Lorentzen[a], Christopher Bronk Ramsey[b], David Chivall[b], A. J. Timothy Jull[c,d,e], and Todd E. Lange[d]

[a]Cornell Tree Ring Laboratory, Department of Classics, Cornell University, Ithaca, NY 14853; [b]Research Laboratory for Archaeology, School of Archaeology, OX1 3TG Oxford, United Kingdom; [c]Department of Geosciences, University of Arizona, Tucson, AZ 85721; [d]University of Arizona Accelerator Mass Spectrometry Laboratory, University of Arizona, Tucson, AZ 85721; and [e]Isotope Climatology and Environmental Research Centre, Institute of Nuclear Research, 4026 Debrecen, Hungary

Edited by Edouard Bard, Centre Européen de Recherche et d'Enseignement des Géosciences de l' Environnement, Aix-en-Provence, France, and accepted by Editorial Board Member Thure E. Cerling May 6, 2018 (received for review November 7, 2017)

Considerable work has gone into developing high-precision radiocarbon (^{14}C) chronologies for the southern Levant region during the Late Bronze to Iron Age/early Biblical periods (~1200–600 BC), but there has been little consideration whether the current standard Northern Hemisphere ^{14}C calibration curve (IntCal13) is appropriate for this region. We measured ^{14}C ages of calendar-dated tree rings from AD 1610 to 1940 from southern Jordan to investigate contemporary ^{14}C levels and to compare these with IntCal13. Our data reveal an average offset of ~19 ^{14}C years, but, more interestingly, this offset seems to vary in importance through time. While relatively small, such an offset has substantial relevance to high-resolution ^{14}C chronologies for the southern Levant, both archaeological and paleoenvironmental. For example, reconsidering two published studies, we find differences, on average, of 60% between the 95.4% probability ranges determined from IntCal13 versus those approximately allowing for the observed offset pattern. Such differences affect, and even potentially undermine, several current archaeological and historical positions and controversies.

radiocarbon | calibration | radiocarbon offsets | southern Levant | archaeology

A long-standing assumption on theoretical and empirical grounds holds that, because of rapid mixing (on the order of less than a month), the premodern atmospheric radiocarbon (^{14}C) levels for the midlatitudes are effectively uniform on an annual basis for each hemisphere, thus permitting use of standard northern and southern hemisphere ^{14}C calibration curves for the Holocene (1–4). However, a number of investigations indicate possible spatial variations in contemporary ^{14}C levels (5–9). There are indications that such regional ^{14}C offsets, in some cases, show temporal variability associated with fluctuations in climate processes and changes in solar activity and ocean circulation (6, 9). Observed regional offsets are typically linked either with changing impacts of ^{14}C reservoirs on an area over time, as in the case of East Asia (8, 9), or with differences in the timing of growing seasons for plants, and hence $^{14}CO_2$ uptake within a hemisphere, leading to the representation of differing parts of the intraannual ^{14}C cycle, in particular when maximized under certain conditions (6, 7, 10–13).

Such offsets have paleoclimate relevance, but they are also of direct archaeological and historical importance. As ^{14}C dating and derived timescales become more precise, potential regional offsets in contemporary ^{14}C levels, and especially the issues of their scale and temporal stability, become relevant to research exploiting the limits of ^{14}C dating resolution. The southern Levant has seen intense research efforts aimed at high-resolution ^{14}C chronologies for the Late Bronze and Iron Ages (~1200–600 BC), some trying to link with early history and Biblical chronology (14–21). Despite large datasets and sophisticated analytical programs, the issue of regional ^{14}C offsets versus the default Northern Hemisphere (NH) standard record of IntCal13 (1) has not been seriously considered for the southern Levant.

Here, we investigate the question of the existence of possible offsets in atmospheric ^{14}C values in the southern Levant over the period AD 1610–1912. We analyze ^{14}C levels in known-age native *Juniperus phoenicea* tree rings across this period, employing a tree-ring chronology constructed from samples from historic structures at Taybet Zaman (TZM) in southern Jordan (~30°15′17″N; 35°27′35″E) (Fig. 1*A*). This tree-ring chronology was cross-dated and securely placed in calendar time, employing standard dendrochronological methods (22, 23), against an existing *J. phoenicea* reference chronology from southern Jordan, dating AD 1469–1995 (24, 25) (*Materials and Methods*, Fig. 1*B*, and *SI Appendix*, section 1, Figs. S1 and S2, and Table S1).

Southern Jordan is part of the midlatitude NH. During the period when ^{14}C released from atmospheric nuclear explosions (bomb ^{14}C) exaggerated contemporary intrahemisphere ^{14}C levels, this area falls in the middle of NH zone 2, well away from the dynamic interface regions around the Intertropical Convergence Zone (26). It would therefore be anticipated that the standard midlatitude NH ^{14}C calibration dataset, IntCal13 (1), should be

Significance

We observe a substantive and fluctuating offset in measured radiocarbon ages between plant material growing in the southern Levant versus the standard Northern Hemisphere radiocarbon calibration dataset derived from trees growing in central and northern Europe and North America. This likely relates to differences in growing seasons with a climate imprint. This finding is significant for, and affects, any radiocarbon application in the southern Levant region and especially for high-resolution archaeological dating—the focus of much recent work and scholarly debate, especially surrounding the timeframe of the earlier Iron Age (earlier Biblical period). Our findings change the basis of this debate; our data point to lower (more recent) ages by variously a few years to several decades.

Author contributions: S.W.M. designed research; S.W.M., C.G., B.L., C.B.R., D.C., A.J.T.J., and T.E.L. performed research; S.W.M., C.G., B.L., C.B.R., D.C., A.J.T.J., and T.E.L. contributed new reagents/analytic tools; S.W.M., C.G., B.L., C.B.R., D.C., A.J.T.J., and T.E.L. analyzed data; and S.W.M., C.G., B.L., C.B.R., D.C., A.J.T.J., and T.E.L. wrote the paper.

The authors declare no conflict of interest.

This article is a PNAS Direct Submission. E.B. is a guest editor invited by the Editorial Board.

[1]To whom correspondence should be addressed. Email: sm456@cornell.edu.

This article contains supporting information online at www.pnas.org/lookup/suppl/doi:10.1073/pnas.1719420115/-/DCSupplemental.

Published online May 29, 2018.

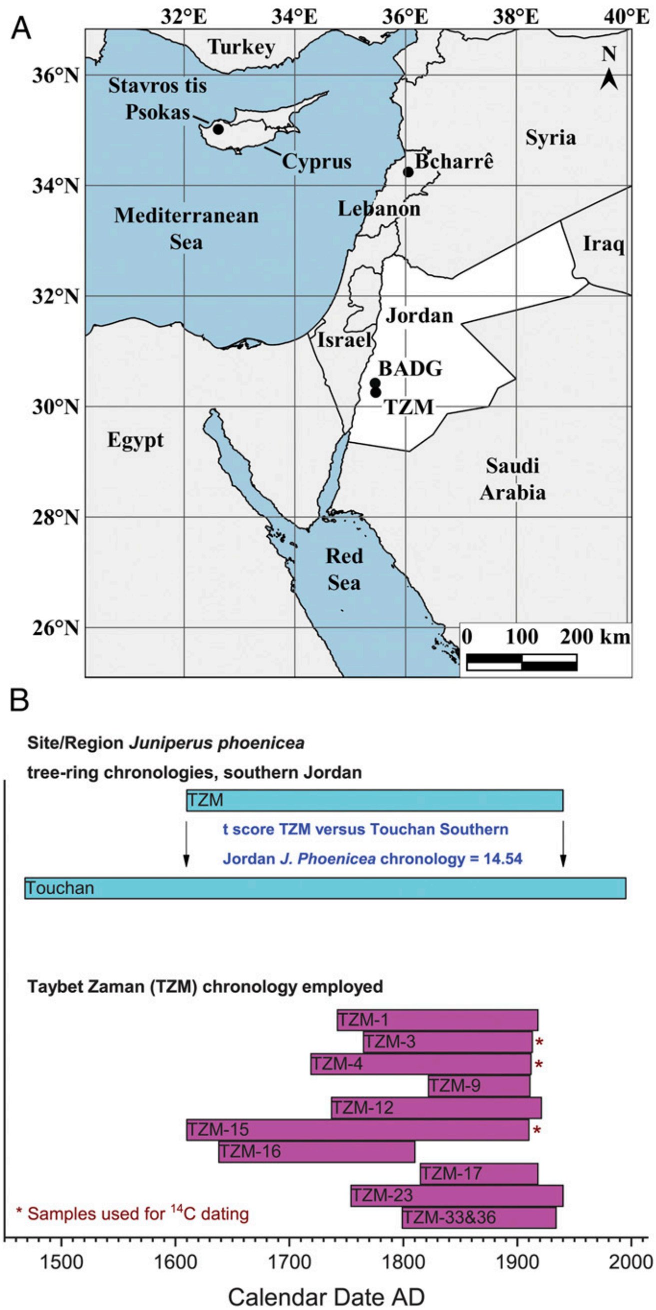

Fig. 1. (*A*) Map showing location of study area and sampled sites, TZM and BADG. (*B*) The time periods covered by the TZM *J. phoenicea* known-age tree-ring chronology and its cross-dating versus the existing chronology (24, 25).

applicable for plant material from southern Jordan, as only during the peak of bomb ^{14}C production, ~AD 1955–1970, does the NH zone 2 region vary from NH zone 1, the source of most of the wood employed to build IntCal13 (central and northern Europe and North America) for the last few thousand years (1, 26). To investigate and test this assumption, we compare ^{14}C ages obtained at the Arizona (AA) and Oxford (OxA) AMS ^{14}C laboratories on known-age 5-y sections of tree rings dissected from the TZM timbers (*SI Appendix*, section 2 and Table S2) with the corresponding values of IntCal13 (1), and also with previous OxA ^{14}C data on known-age plant material from 18th to 19th century AD Egypt which have been argued to demonstrate a 19 ± 5 ^{14}C years offset for plants growing in Egypt in premodern times (7) (Fig. 2).

Results

The Jordanian juniper (JJ) samples, on average, yield older ^{14}C ages compared with the corresponding IntCal13 values (Fig. 2). The average offset for the collected JJ data, calculated as a Delta_R query in OxCal 4.3 (27) versus IntCal13 with curve resolution set at 1 y with a neutral prior of 0 ± 20, yields a posterior of 20.6 ± 4.5 ^{14}C years for the AA data and 19.1 ± 2.8 ^{14}C years for the OxA data (Fig. 2*C*), or 18.6 ± 2.5 ^{14}C years if the OxA and AA datasets are combined (*SI Appendix*, Figs. S3–S5 and Tables S4 and S5). All these values are very comparable with the average 19 ± 5 ^{14}C years offset determined previously for plants growing in Egypt (7, 12). We note that the offsets we observe are represented in data from more than one TZM tree, indicating a general pattern and ruling out any single sample/tree issue (*SI Appendix*, Fig. S6). In addition, by way of independent replication and confirmation, another ordered series of JJ samples from a different location (4 km NNW of Al-Bayda, site code BADG, ~30°25′18″N, 35°26′58″E) (Fig. 1*A*) also exhibit similar and contemporary ^{14}C offsets versus IntCal13 (*SI Appendix*, sections 1 and 2 and Figs. S7–S17).

However, importantly, it is also evident that this ^{14}C offset appears to fluctuate over time (Fig. 2 *A* and *B* and *SI Appendix*, Figs. S3, S5, S6, and S8–S10). Thus, while real and relevant for ^{14}C dating and analysis in the southern Levant, this situation also suggests that it is likely inappropriate to consider any average offset value, or potential correction, as generally relevant or

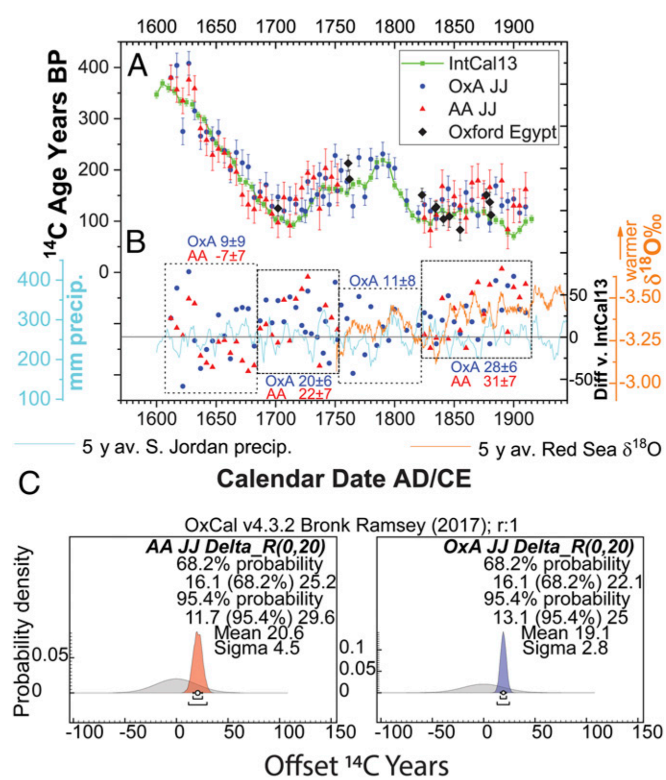

Fig. 2. (*A*) The ^{14}C ages from the known-age JJ samples, and previously published dates on known-age annual plant matter from Egypt (7), plotted against the NH radiocarbon calibration curve (IntCal13) (1) (1σ errors shown). (*B*) Differences between the JJ ^{14}C ages and IntCal13 and comparison of these trends versus 5-y moving averages of reconstructed precipitation for southern Jordan (24) and regional temperature from Red Sea corals (28). (*C*) Overall offsets in ^{14}C ages between the JJ samples and IntCal13 by laboratory, showing (light gray) the neutral prior (0 ± 20) versus the calculated posterior densities from each laboratory's data versus IntCal13 (red and blue regions) (27).

applicable for any specific period without having data available for that specific time interval. While no correlation of the changing offset is evident with reconstructed precipitation for southern Jordan (24), there do appear associations between an increased offset and warmer temperatures as reconstructed from Red Sea corals in the period after ∼AD 1835 (28) (Fig. 2*B*), or generally for the extratropical NH (29), and with reversals in IntCal13 which correspond to increased solar irradiance (1, 3, 6, 29) (Fig. 2*A* and *SI Appendix*, Figs. S3, S6, and S8–S10). The offset period ∼1685–1762 (Fig. 2 and *SI Appendix*, Fig. S3), for example, starts around the change from the cool and (in the Mediterranean) dry conditions in the 17th century leading to the Maunder Minimum (peak 1645–1700), and corresponds especially to the warmer, post-Maunder Minimum conditions, particularly the long, stable, wetter period ∼1700–1750 noted in much of the Mediterranean (30). Despite expected variability in the ^{14}C measurements of the AA versus OxA laboratories on the same material, the fluctuating offset is clear, independently, in the data from both laboratories. The boxes illustrated in Fig. 2*B* offer a subjective breakup of the data, indicating four possible time divisions, with two boxes offering little significant average offset and two boxes indicating a significant offset. With one partial exception, at AD 1855, the OxA ^{14}C data on known-age annual plant material from Egypt produced similar age estimates (and, even for the 1855 exception, the JJ data from both AA and OxA show a consonant shift to more recent ^{14}C ages centered at this year). The JJ ^{14}C ages for some periods compare very well with values from the Southern Hemisphere (SH) ^{14}C calibration dataset, SHCal13 (2) (Fig. 3*A*). On average, the JJ ^{14}C data lie midway between the NH and SH ^{14}C calibration curves, with offsets around half the average interhemispheric offset of 43 ± 23 ^{14}C years (2) (Figs. 2 and 3*A*). Laboratory quality controls at both the AA and OxA laboratories (*SI Appendix*, section 2) and the dating of other known age samples indicate good agreement and only negligible differences for midlatitude NH samples with IntCal13 for both AA (31, 32) and OxA (Fig. 3 *B* and *C* and *SI Appendix*, Figs. S18 and S19) (33). Thus, the consistent and fluctuating ^{14}C offsets observed for these JJ samples by both the AA and OxA laboratories versus IntCal13 appear real.

Discussion

The explanation proposed for the observed Egyptian offset (7, 12) was the different, almost opposite, growing season (winter to spring) for plants in Egypt in antiquity (before the Aswan Dam constructions in the 20th century AD) versus the spring and especially summer growing season for the central and northern European and northern North American trees comprising the Holocene IntCal13 dataset (1, 34). Since these near-opposite growing seasons correspond to periods of peak variability in natural (premodern) intraannual ^{14}C level fluctuations, growing-season variability could readily account for the ∼2.5‰ ^{14}C offset observed for Egypt (6, 7, 13, 34–38). Juniper trees in southern Jordan grow from autumn to early summer (24, 25), also largely in antiphase with trees in central and northern Europe and northern North America. In contrast, ^{14}C ages on known-age wood from conifer trees growing at higher elevations in the northern Levant (Bcharrê, northern Lebanon), western Cyprus (Stavros tis Psokas), and western Turkey, which have growing seasons spanning, variously, from spring to summer (depending on temperature and moisture availability) (39–43), typically show no measureable offset (6, 44), even when the Jordanian trees are exhibiting larger offsets from IntCal13 (e.g., AD 1685–1760, 1835–1910) (Fig. 3*A*).

If we consider the plant taxa typically recovered from archaeological contexts in the southern Levant and subject to ^{14}C dating, these have traditional growing seasons (subject to some intraregional geographic variations). Whereas a first group of crops comprising wheat, barley, oats, peas, lentils, and vetch grow winter to spring (with harvest April to May), a second group comprising chickpeas, sesame, flax, millet and some grapes, figs, and pomegranates grow later (harvest June to August), and a third group comprising other grapes, figs, pomegranates, and olives grow after that (harvest September through November; e.g., olives flower April to May, fruit grows in the summer, and harvest is around November) (45). Thus, a growing-season–related ^{14}C offset versus central and northern Europe should apply to the first group, but not the second group, and then apply again, partially to more fully, to the third group. The growth periods for native tree species contributing charcoal at archaeological sites in the southern Levant likewise vary, but the typical pattern sees a period of dormancy over the hot, dry, summer months (42), so much of the growing season will be out of phase with central and northern European oak trees. If we examine the 121 ^{14}C dates listed in one major study on Iron Age Israel as representative (17), 44% are on seeds/grains/semolina, 33% are on olive pits, 22% are on charcoal, and just 1% are on grapes. Thus, the majority of these samples likely fall outside the main spring to summer growing season represented by central and northern European oaks (46)–source of the earlier first millennium BC calibration data (1)–and so would be affected by a growing-season ^{14}C offset.

However, a systematic growing-season–related ^{14}C offset seems unlikely to be the sole explanation for the JJ ^{14}C data, since the

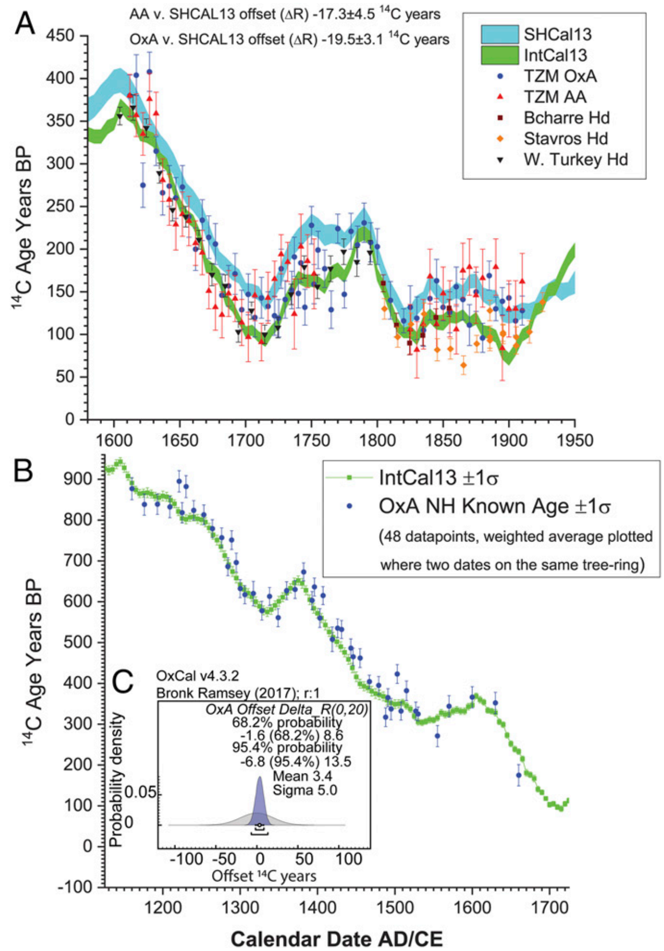

Fig. 3. (*A*) Comparison of the JJ ^{14}C data by laboratory versus both IntCal13 (1) and SHCal13 (2) (1σ errors shown). Known-age tree-ring ^{14}C measurements from Bcharrê, (northern Lebanon), Stavros tis Psokas (western Cyprus), and Çatacık (western Turkey), are also shown (44). (*B*). OxA data on other known age NH tree rings (61, 62) versus IntCal13 (1). (*C*) Overall ^{14}C years offset OxA NH data in *B* versus IntCal13; light gray region shows the neutral prior (0 ± 20) versus the calculated posterior region (blue) (27).

offset appears to vary over time from significant to insignificant values. The offset trend is most clear during regional warming periods, e.g., after AD 1835 (28) (Fig. 2*B*), or in the period following the Maunder Minimum (~AD 1700–1750) (in *Results*). Such changes in climate likely modified the local growing season. For example, warmer conditions probably brought both the start and end of the growing season forward in the southern Levant, exaggerating the growing-season offset versus central and northern Europe. An increased scale of observed offset from the early 20th century might be associated with the increased Suess effect from fossil fuel use evident over Europe from about this time (47) (and thence transport to the East Mediterranean), especially since the Suess effect, which produces older observed ^{14}C ages, peaks on an intraannual basis in the winter months for the NH (34, 35, 48). It would thus be reflected in the JJ wood growing across the winter months, and act to exaggerate differences in ^{14}C values within the NH when compared with wood reflecting spring and especially summer ^{14}C values, as IntCal13 comprises (1), when the Suess effect is at its annual minimum. However, the larger offsets observed in our data in the mid to later 19th century (Fig. 2*B* and *SI Appendix*, Fig. S3) occur before any plausible Suess effect and therefore likely reflect natural processes.

Our finding of a fluctuating ^{14}C offset for the southern Levant versus IntCal13 (1) (and so against the IntCal13 ^{14}C record from central and northern European and North American wood) potentially complicates previous studies where average offsets identified from particular periods or sets of samples were then considered as generally relevant through time, in particular in the case of Egypt (e.g., refs. 7 and 12). Instead, in cases like the southern Levant, where there appears to be a potential substantive growing-season (or other) difference which may provide a basis for intraannual offsets in ^{14}C values as recorded in plant matter, our dataset indicates the need for a regional calibration time series if appropriate corrections are to be made for any particular time interval. Where such calibration time series are not yet available (namely, before AD 1610 for the southern Levant case at present), our dataset better indicates the circumstances under which a likely potential range of error may apply for earlier periods—assuming that similar conditions and process apply in earlier periods and accepting some possible variations—rather than offering any specific average correction factor. If we consider the combined OxA and AA dataset in Fig. 2*A* (as in *SI Appendix*, Fig. S3), then, overall, the offset is around 19 ± 3 ^{14}C years (*SI Appendix*, Fig. S4*A*) applying an OxCal Delta_R calculation (27) with a neutral prior of 0 ± 20, or 16 ± 5 ^{14}C years comparing observed values versus (linear interpolated) IntCal13 (1) values and errors (so around 2 to 2.5‰). These values and the ones for the separate OxA and AA datasets (Fig. 2*C*) are all strikingly similar to the 19 ± 5 ^{14}C years offset observed previously from plant material from Egypt (7, 12). Where an offset applies, this suggests the approximate scale of a likely minimum southern Levant offset. However, the offset between the JJ and IntCal13 across two (subjectively selected) intervals with larger apparent offsets, between AD 1685–1762 and between AD 1818–1912, is a little larger at about 24 ± 5 ^{14}C years (*SI Appendix*, Fig. S5), or around 3‰. Such possible offsets (or intraannual variations) of, overall, around 2 to 3‰ are plausible in terms of the known cycle and scale of natural premodern (preindustrial) intraannual ^{14}C variations (7, 13, 34–38). Our findings highlight that it is important now to extend the time period of comparison if we are to determine whether such a scale of offset for the southern Levant occurs regularly at times when there are reversals and plateaus in the ^{14}C calibration curve and/or regional or wider general warming episodes. On the basis of the currently available comparison, AD 1610–1910, we might anticipate the possibility of offsets relevant to ^{14}C dating in the southern Levant ranging from about 19 ± 5 ^{14}C years to 24 ± 5 ^{14}C years at such times.

The findings reported here have immediate implications for high-resolution archaeological dating in the southern Levant. If the period AD 1610–1910 is representative in terms of a fluctuating offset versus the NH IntCal13 dataset, then, for substantial periods, and especially those where there are reverses or plateaus in the ^{14}C calibration curve and/or a local or wider warming climate regime, there is likely a small, fluctuating, but substantive ^{14}C offset in operation in the southern Levant which is of relevance to ^{14}C dating. The impact on archaeological and other ^{14}C dating will vary over time because this offset appears to fluctuate and because of the shape of the ^{14}C calibration curve (1). To explore the potential scale of this issue, based on our JJ dataset (Fig. 2*A* and *SI Appendix*, Figs. S3–S5), we consider a possible modification of the IntCal13 ^{14}C calibration curve (1) for the period ~1200–700 BC, covering the debated Iron Age chronology period in the southern Levant. We apply the average 24 ± 5 ^{14}C years adjustment observed across the periods exhibiting a substantive offset in our dataset (*SI Appendix*, Fig. S5) to those parts of the IntCal13 curve

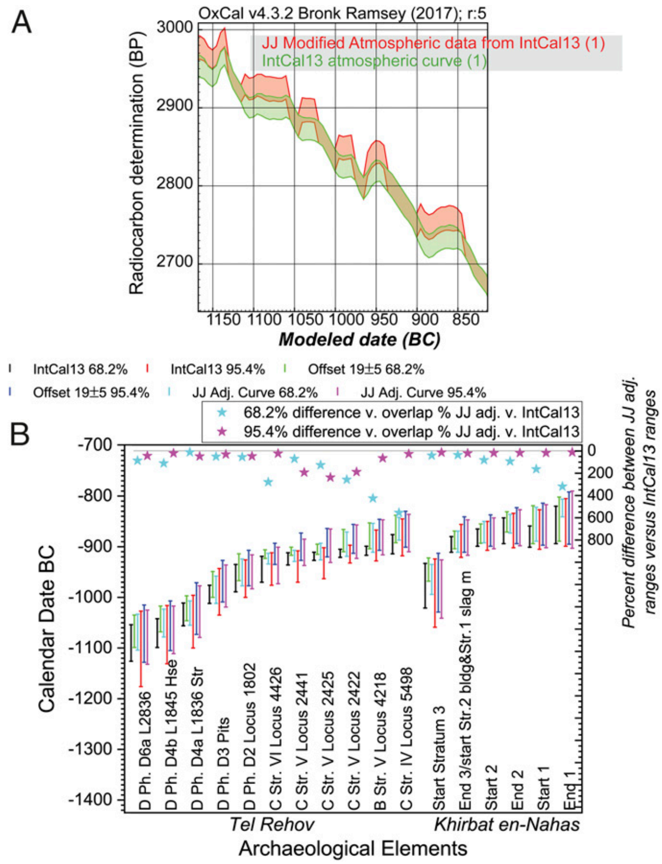

Fig. 4. (*A*) IntCal13 ^{14}C calibration curve ~1200–700 BC approximately adjusted by 24 ± 5 ^{14}C years in the periods where curve taphonomy suggests a substantive JJ offset might apply based on Fig. 2 and *SI Appendix*, Fig. S3 (27). (*B*) (*Bottom*, vertical bars) Comparison of the calibrated calendar age ranges at 68.2% and 95.4% probability with, and without, both the average 19 ± 5 ^{14}C years offset or the approximate JJ adjusted IntCal13 ^{14}C calibration curve for the date sets from Tel Rehov (14) modeled as a sequence in OxCal (27), and the boundaries labeled as indicated from a rerun of the Bayesian chronological model from Khirbat en-Nahas (18). (*Top*, stars) Comparison of the noncommon (nonoverlapping), versus common (overlapping) ranges calculated when comparing the JJ adjusted ranges versus those from IntCal13 expressed as a percentage value: 0% (gray line) equates to exactly the same ranges; the larger percentage numbers indicate progressively less overlap. The average differences across the 17 comparisons are (*i*) for the 68.2% most likely ranges = 162% and (*ii*) for the 95.4% most likely ranges = 60%.

which exhibit reversals or plateaus in ^{14}C values (Fig. 4*A*). Needless to say, this is an approximate and subjective adjustment; the exercise is aimed to be indicative and not robust.

The potential impact of these offsets on real archaeological cases is then illustrated by looking at the changes in calendar date ranges achieved with, versus without, these offsets (Fig. 4*A*) in two high-profile examples: the initial dating of Tel Rehov in northern Israel, central to the early Iron Age and history debate in Israel (14), and the dating of Khirbat en-Nahas in southern Jordan, central to redating the rise of Iron Age Edom (18). The dates are on cereals, olive pits, seeds, and (in one case) charcoal for Tel Rehov, and charcoal and seeds (*Phoenix dactylifera*) for Khirbat en-Nahas, and all should likely reflect any contemporary southern Levant ^{14}C offset. We model the published Tel Rehov ^{14}C dates (minus the calendar date estimates) as a sequence in OxCal (27) with, and without, the above offsets, and, for Khirbat en-Nahas, we rerun the published Bayesian dating model with, and without, the above offsets (Fig. 4*B* and *SI Appendix*, section 2 and Tables S6 and S7). To compare the relevance of determining a specific record of such offsets through time, versus merely applying a general average (Delta_R) correction, we also consider the same data but applying a general 19 ± 5 ^{14}C years Delta_R correction (as, e.g., refs. 7 and 12). The calibrated calendar age ranges for the elements of the Tel Rehov and Khirbat en-Nahas site sequences are shown from the nonmodified IntCal13 dataset, with the general 19 ± 5 ^{14}C years correction, and with the specific contextualized approximate/estimated southern Levant modified calibration curve (Fig. 4*A*) in Fig. 4*B*.

It is notable that there is variation, and, in a number of cases, considerable variation, in the most likely 68.2% ranges, comparing the IntCal13 ranges with either the general 19 ± 5 ^{14}C years adjustment or the data from the estimated JJ adjusted calibration curve. The 17 cases shown highlight that the application of a general 19 ± 5 ^{14}C years offset tends to create larger differences in most cases (in 76% versus 24% of cases) versus the JJ adjusted curve, which tries better to model a plausible fluctuating scenario in keeping with observed data AD 1610–1910. This situation highlights the likely problems created if a simple "average" correction is applied to a geographic area when, in fact, the offset in question appears to fluctuate through time. Regardless, however, we may note that every shift is to "lower" or more recent calendar age ranges (whichever adjustment is considered), which is significant when considering recent debates over absolute dates for the Iron Age archaeological periods in the southern Levant. If we compare the 95.4% probability ranges, there are, in several cases, greater overlaps, but, even so, in a number of cases, there are substantial differences, and again the shifts are to lower or more recent calendar ages compared with the nonmodified IntCal13 ranges. If we consider the Fig. 4*B* comparisons between the IntCal13 ranges and the JJ adjusted ranges (comparing the calendar range of overlap versus the calendar years of nonoverlap between the IntCal13 and JJ adjusted curve ranges: Fig. 4*B*, *Top*, stars), then 14 of 17 (82%) of the most likely 68.2% probability ranges vary by ≥50%, and 12 of 17 (71%) of the most likely 95.4% ranges vary by ≥20%. While not always large, the scale of variations evident in many cases is sufficient to be substantive in considerations of Iron Age chronology, especially as current debates over Iron Age chronology in the southern Levant focus on intervals of only a few decades to ∼50 y to 100 y (13–20, 49, 50).

Available paleoclimate data for the southern Levant for the earlier Iron Age are inconclusive, but, after indications of cooler and arid conditions in the period around the close of the Late Bronze Age through initial Iron Age ∼3300–3000 BP (51–55), there are some (not always consistent) suggestions of wetter and/or warming conditions and increased solar irradiance ∼3000–2800 BP in the East Mediterranean region (refs. 52, 54, and 56–58; note that we adjust the ref. 57 timescale following their maximum age correction to match the age of the Santorini eruption as in ref. 53). This might suggest some exaggeration of regional growing-season ^{14}C offsets in this period, especially around the plateau/reversal in the ^{14}C record ∼2850–2800 BP/900–850 BC (1), and hence that a larger offset, at least comparable to those identified in the recent periods ∼AD 1685–1762 and AD 1818–1912, is relevant.

Although, overall, the ^{14}C offset identified here produces what may seem to be relatively small dating changes, these are revealed to be of a scale that is important for high-resolution chronological work. They are especially important for the contested and detailed chronology debates in archaeological scholarship on the southern Levant region, particularly for those focused on differences of only a few decades to ∼50 y to 100 y in recent "high" (or conventional) versus "low" chronology debates (13–20, 49, 50). Thus, we recommend that users must proceed with caution when dating plant material from the southern Levant with a winter to spring growing season. It also seems likely that the offset we observe fluctuates, and thus is not best compensated for via a static, systematic, adjustment. This potentially complicates the previously proposed Egyptian offset (7, 12). The offset we observe is also relevant to other high-resolution work in the southern Levant based on detailed ^{14}C chronology, such as paleoenvironmental investigations (52, 54), or for the correct association of radiocarbon-dated contexts and time series with geomagnetic intensity series which show important changes in the earlier Iron Age period in the southern Levant region (59, 60). The growing season (and climate) related ^{14}C offset we identify changes and undermines the basis and assumptions in existing ^{14}C work in the southern Levant, and especially in those periods where a larger offset likely applies. In these cases, the effect of the offset can be substantial, and of the scale of the existing range of scholarly debate. This ^{14}C offset therefore requires attention, and, in particular, further work is necessary to better define its history since it appears to be time-varying (likely with climate associations as these affect growing seasons), especially when attempting to integrate ^{14}C chronology closely with history. Ideally, a southern Levant radiocarbon calibration curve is required, or at least a longer comparison curve. The ^{14}C offset observed in this study highlights a topic of general relevance to the radiocarbon field in cases where, within the same hemisphere, there are substantial differences in growing seasons (and hence conditions) for plants compared with the standard growing season represented by the midlatitude IntCal13 (1) ^{14}C calibration dataset. In the present case, for example, the offset observed points toward more recent (lower) age ranges being more likely for some intervals in the earlier Iron Age in the Southern Levant, but for reasons not currently discussed in the high versus low scholarly debate.

Materials and Methods

We sampled native juniper (*J. phoenicea*) timbers in historical structures at TZM in southern Jordan (∼30°15′17″N; 35°27′35″E) (Fig. 1*A* and *SI Appendix*, sections 1 and 4). Employing standard dendrochronological methods (22, 23), the TZM historical timbers were cross-dated and placed in absolute calendar time, AD 1610–1940, against an existing *J. phoenicea* reference chronology from southern Jordan, dating AD 1469–1995 (24, 25) (Fig. 1*B* and *SI Appendix*, section 1, Figs. S1 and S2, and Table S1). Known-age 5-y sections of the TZM tree rings were dissected with a steel blade under a binocular microscope from the TZM timbers for ^{14}C dating at the AA and OxA accelerator mass spectrometry (AMS) ^{14}C laboratories (*SI Appendix*, section 2 and Table S2). A sequence of ordered, but not known-age, tree-ring samples from the BADG site (∼30°25′18″N, 35°26′58″E) (Fig. 1*A*) were also dated at the AA and OxA AMS ^{14}C laboratories (*SI Appendix*, section 2 and Table S3). The resultant ^{14}C ages were then compared against IntCal13 (1) (e.g., *SI Appendix*, Table S4), and also OxA data on known age plant material from 18th to 19th century AD Egypt which have been argued to demonstrate a 19 ± 5 ^{14}C years offset for plants growing in Egypt in premodern times (7) (Fig. 2 and *SI Appendix*, Figs. S3, S5, S6, and S8–S13). Where stated (in the text, or where a figure plot indicates "r:1" at the top), the five-calendar-year resolution IntCal13 record was modeled to one-calendar year resolution by linear interpolation. Analysis of the ^{14}C data employed the OxCal software (27) version 4.3. The OxCal runfiles with the data and coding employed for Fig. 4*B* are listed in *SI Appendix*, Tables

EARTH, ATMOSPHERIC, AND PLANETARY SCIENCES

ANTHROPOLOGY

S6 and S7, and the OxCal runfile for the analyses in *SI Appendix*, Figs. S8 and S11 are in *SI Appendix*, Table S5. As an example (employing the relevant data in *SI Appendix*, Table S2), the OxCal runfile for the analysis shown of the OxA data in Fig. 2*C* is listed at *SI Appendix*, Table S8.

ACKNOWLEDGMENTS. We thank Linah Ababneh for organizing access and for fieldwork collaboration and for work on the BADG-1 sample, Ameen Al-Duqs and the Jordanian Ministry of Agriculture for fieldwork collaboration and permissions, Kate Seufer and Cynthia Kocik for laboratory and technical assistance, and Pierre M. Bikai for access to some samples. We thank the reviewers. We thank the laboratory teams at the Arizona and Oxford Radiocarbon Laboratories, and the American Center of Oriental Research, Amman. We thank the former Hotel Taybet Zaman (now Hyatt Zaman Hotel & Resort). This work was supported by the National Science Foundation, Award BCS 1219315; the Social Science and Humanities Research Council, Canada, via the CRANE project, University of Toronto, Award 895-2011-1026; and the College of Arts & Sciences and the Department of Classics, Cornell University.

1. Reimer PJ, et al. (2013) IntCal13 and Marine13 radiocarbon age calibration curves 0-50,000 years cal BP. *Radiocarbon* 55:1869–1887.
2. Hogg AG, et al. (2013) SHCal13 southern hemisphere calibration, 0-50,000 years cal BP. *Radiocarbon* 55:1889–1903.
3. Stuiver M, Braziunas TF (1998) Anthropogenic and solar components of hemispheric ^{14}C. *Geophys Res Lett* 25:329–332.
4. Braziunas TF, Fung IY, Stuiver M (1995) The preindustrial atmospheric $^{14}CO_2$ latitudinal gradient as related to exchanges among atmospheric, oceanic, and terrestrial reservoirs. *Global Biogeochem Cycles* 9:565–584.
5. McCormac FG, Baillie MGL, Pilcher JR, Kalin RM (1995) Location-dependent differences in the ^{14}C content of wood. *Radiocarbon* 37:395–407.
6. Kromer B, et al. (2001) Regional $^{14}CO_2$ offsets in the troposphere: Magnitude, mechanisms, and consequences. *Science* 294:2529–2532.
7. Dee MW, et al. (2010) Investigating the likelihood of a reservoir offset in the radiocarbon record for ancient Egypt. *J Archaeol Sci* 37:687–693.
8. Hong W, et al. (2013) Regional offset of radiocarbon concentration and its variation in the Korean atmosphere from AD 1650-1850. *Radiocarbon* 55:753–762.
9. Nakamura T, Masuda K, Miyake F, Nagaya K, Yoshimitsu T (2013) Radiocarbon ages of annual rings from Japanese wood: Evident age offset based on IntCal09. *Radiocarbon* 55:763–770.
10. Manning SW, Kromer B, Kuniholm PI, Newton MW (2001) Anatolian tree rings and a new chronology for the east Mediterranean Bronze-Iron Ages. *Science* 294: 2532–2535.
11. Dellinger F, et al. (2004) A ^{14}C calibration with AMS from 3500 to 3000 BC, derived from a new high-elevation stone-pine tree-ring chronology. *Radiocarbon* 46:969–978.
12. Bronk Ramsey C, et al. (2010) Radiocarbon-based chronology for dynastic Egypt. *Science* 328:1554–1557.
13. Manning SW, et al. (2014) High-precision dendro-^{14}C dating of two cedar wood sequences from First Intermediate Period and Middle Kingdom Egypt and a small regional climate-related ^{14}C divergence. *J Archaeol Sci* 46:401–416.
14. Bruins HJ, van der Plicht J, Mazar A (2003) ^{14}C dates from Tel Rehov: Iron-Age chronology, pharaohs, and Hebrew kings. *Science* 300:315–318.
15. Levy TE, Higham T, eds (2005) *The Bible and Radiocarbon Dating: Archaeology, Text and Science* (Equinox, London).
16. Sharon I, Gilboa A, Jull T, Boaretto E (2007) Report on the first stage of the Iron Age dating project in Israel: Supporting the low chronology. *Radiocarbon* 49:1–46.
17. Mazar A, Bronk Ramsey C (2008) ^{14}C dates and the Iron Age chronology of Israel: A response. *Radiocarbon* 50:159–180.
18. Levy TE, et al. (2008) High-precision radiocarbon dating and historical biblical archaeology in southern Jordan. *Proc Natl Acad Sci USA* 105:16460–16465.
19. Finkelstein I, Piasetzky E (2010) Radiocarbon dating the Iron Age in the Levant: A Bayesian model for six ceramic phases and six transitions. *Antiquity* 84:374–385.
20. Lee S, Bronk Ramsey C, Mazar A (2013) Iron Age chronology in Israel: Results from modeling with a trapezoidal Bayesian framework. *Radiocarbon* 55:731–740.
21. Boaretto E (2015) Radiocarbon and the archaeological record: An integrative approach for building an absolute chronology for the Late Bronze and Iron Ages of Israel. *Radiocarbon* 57:207–216.
22. Schweingruber FH (1988) *Tree Rings: Basics and Applications of Dendrochronology* (D. Reidel, Dordrecht, The Netherlands).
23. Cook ER, Kairiukstis LA, eds (1990) *Methods of Dendrochronology: Applications in the Environmental Sciences* (Kluwer, Dordrecht, The Netherlands).
24. Touchan R, Meko D, Hughes MK (1999) A 396-year reconstruction of precipitation in southern Jordan. *J Am Water Resour Assoc* 35:49–59.
25. Touchan R, Hughes MK (1999) Dendrochronology in Jordan. *J Arid Environ* 42: 291–303.
26. Hua Q, Barbetti M, Rakowski AR (2013) Atmospheric radiocarbon for the period 1950-2010. *Radiocarbon* 55:2059–2072.
27. Bronk Ramsey C (2009) Bayesian analysis of radiocarbon dates. *Radiocarbon* 51: 337–360.
28. Felis T, et al. (2000) A coral oxygen isotope record from the northern Red Sea documenting NAO, ENSO, and North Pacific teleconnections on Middle East climate variability since the year 1750. *Paleoceanography* 15:679–694.
29. Xing P, et al. (2016) The extratropical northern hemisphere temperature reconstruction during the last millennium based on a novel method. *PLoS One* 11: e0146776.
30. Nicault A, et al. (2008) Mediterranean drought fluctuation during the last 500 years based on tree-ring data. *Clim Dyn* 31:227–245.
31. Jull AJT, et al. (2014) Excursions in the ^{14}C record at A.D. 774–775 in tree rings from Russia and America. *Geophys Res Lett* 41:3004–3010.
32. Miyake F, et al. (2017) Large ^{14}C excursion in 5480 BC indicates an abnormal sun in the mid-Holocene. *Proc Natl Acad Sci USA* 114:881–884.
33. Marshall P, et al. (2018) ^{14}C wiggle-matching of short tree-ring sequences from post-medieval buildings in England. *Nucl Instrum Methods Phys Res B*, in press.
34. Levin I, Kromer B (1997) Twenty years of atmospheric $^{14}CO_2$ observations at Schauinsland Station, Germany. *Radiocarbon* 39:205–218.
35. Levin I, Kromer B (2004) The tropospheric $^{14}CO_2$ level in mid-latitudes of the northern hemisphere (1959–2003). *Radiocarbon* 46:1261–1272.
36. Levin I, et al. (1992) Radiocarbon in atmospheric carbon dioxide and methane: Global distribution and trends. *Radiocarbon After Four Decades: An Interdisciplinary Perspective*, eds Taylor RE, Long A, Kra RS (Springer, New York), pp 503–518.
37. Levin I, Hesshaimer V (2000) Radiocarbon–A unique tracer of global carbon cycle dynamics. *Radiocarbon* 42:69–80.
38. Randerson JT, Enting IG, Schuur EAG, Caldeira K, Fung IY (2002) Seasonal and latitudinal variability of troposphere $\Delta^{14}CO_2$: Post bomb contributions from fossil fuels, oceans, the stratosphere, and the terrestrial biosphere. *Global Biogeochem Cycles* 16: 1112.
39. Güney A, Küppers M, Rathberger C, Şahin M, Zimmermann R (2017) Intra-annual stem growth dynamics of Lebanon Cedar along climatic gradients. *Trees* 31:587–606, and erratum (2017) 31:1375.
40. De Luis M, Gricar J, Cufar K, Raventós J (2007) Seasonal dynamics of wood formation in *Pinus halepensis* from dry and semi-arid ecosystems in Spain. *IAWA J* 28:389–404.
41. Köse N, Akkemik Ü, Dalfes HN, Özeren MS, Tolunay D (2012) Tree-ring growth of *Pinus nigra* Arn. subsp. *pallasiana* under different climate conditions throughout western Anatolia. *Dendrochronologia* 30:295–301.
42. Liphschitz N, Lev-Yadun S (1986) Cambial activity of evergreen and seasonal dimorphics around the Mediterranean. *IAWA J* 7:145–153.
43. Vicente-Serrano SM, et al. (2013) Response of vegetation to drought time-scales across global land biomes. *Proc Natl Acad Sci USA* 110:52–57.
44. Manning SW, Kromer B (2012) Considerations of the scale of radiocarbon offsets in the east Mediterranean, and considering a case for the latest (most recent) likely date for the Santorini eruption. *Radiocarbon* 54:449–474.
45. Borowski O (1987) *Agriculture in Iron Age Israel* (Eisenbrauns, Winona Lake, IN).
46. Eckstein D (2007) Human time in tree rings. *Dendrochronologia* 24:53–60.
47. de Jong AFM, Mook WG (1982) An anomalous Suess effect above Europe. *Nature* 298: 641–644.
48. Levin I, Schuchard J, Kromer B, Münnich KO (1989) The continental European Suess effect. *Radiocarbon* 31:431–440.
49. Finkelstein I, Piasetzky E (2011) The Iron Age chronology debate: Is the gap narrowing? *Near East Archaeol* 74:50–54.
50. Mazar A (2011) The Iron Age chronology debate: Is the gap narrowing? Another viewpoint. *Near East Archaeol* 74:105–111.
51. Drake BL (2012) The influence of climatic change on the Late Bronze Age collapse and the Greek Dark Ages. *J Archaeol Sci* 39:1862–1870.
52. Langgut D, Finkelstein I, Litt T, Neumann FH, Stein M (2015) Vegetation and climate changes during the Bronze and Iron Ages (∼3600-600 BCE) in the southern Levant based on palynological records. *Radiocarbon* 57:217–235.
53. Knapp AB, Manning SW (2016) Crisis in context: The end of the Late Bronze Age in the eastern Mediterranean. *Am J Archaeol* 120:99–149.
54. Neugebauer I, et al. (2015) Evidences for centennial dry periods at ∼3300 and ∼2800 cal. Yr BP from micro-facies analyses of the Dead Sea sediments. *Holocene* 25: 1358–1371.
55. Finkelstein I, Langgut D, Meiri M, Sapir-Hen L (2017) Egyptian imperial economy in Canaan: Reaction to the climate crisis at the end of the Late Bronze Age. *Ägypten Levante* 27:249–259.
56. Finné M, Holmgren K, Sundqvist HS, Weiberg E, Lindblom M (2011) Climate in the eastern Mediterranean, and adjacent regions, during the past 6000 years–A review. *J Archaeol Sci* 38:3153–3173.
57. Rohling EJ, Mayewski PA, Hayes A, Abu-Zied RH, Casford JSL (2002) Holocene atmosphere-ocean interactions: Records from Greenland and the Aegean Sea. *Clim Dyn* 18:587–593.
58. Constantin S, Bojar AV, Lauritzen SE, Lundberg J (2007) Holocene and Late Pleistocene climate in the sub-Mediterranean continental environment: A speleothem record from Poleva Cave (Southern Carpathians, Romania). *Palaeogeogr Palaeoclimatol Palaeoecol* 243:322–338.
59. Shaar R, et al. (2016) Large geomagnetic field anomalies revealed in Bronze to Iron Age archeomagnetic data from Megiddo and Tel Hazor, Israel. *Earth Planet Sci Lett* 442:173–185.
60. Ben-Yosef E, Millman M, Shaar R, Tauxe L, Lipschits O (2017) Six centuries of geomagnetic intensity variations recorded by royal Judean stamped jar handles. *Proc Natl Acad Sci USA* 114:2160–2165.
61. Tyers C, et al. (2009) Wiggle-matching using known-age pine from Jermyn Street, London. *Radiocarbon* 51:385–396.
62. Bayliss A, et al. (2017) Informing conservation: Towards ^{14}C wiggle-matching of short tree-ring sequences from medieval buildings in England. *Radiocarbon* 59:985–1007.